ISSN 1674-1056
http://cpb.iphy.ac.cn
http://iopscience.iop.org/cpb
中国物理 B
Chinese Physics
中国物理 Chinese Physics B

Effect of different bending shapes on thermal properties of flexible light-emitting diode filament

Liping Wang(王立平), Wenbo Li(李文博), Yichao Xu(徐一超), Bobo Yang(杨波波), Mingming Shi(石明明), Jun Zou(邹军), Yang Li(李杨), Xinglu Qian(钱幸璐), Fei Zheng(郑飞), Lei Yang(杨磊)

Citation: Chin. Phys. B . 2018, 27(11): 110701. **doi:** 10.1088/1674-1056/27/11/110701

Journal homepage: http://cpb.iphy.ac.cn; http://iopscience.iop.org/cpb

What follows is a list of articles you may be interested in

High-pressure synergetic measurement station (HP-SymS)

Xiaohui Yu(于晓辉), Fangfei Li(李芳菲), Yonghao Han(韩永昊), Fang Hong(洪芳), Changqing Jin(靳常青), Zhi He(何志), Qiang Zhou(周强)

Chin. Phys. B . 2018, 27(7): 070701. **doi:** 10.1088/1674-1056/27/7/070701

A slope-based decoupling algorithm to simultaneously control dual deformable mirrors in a woofer-tweeter adaptive optics system

Tao Cheng(程涛), Wenjin Liu(刘文劲), Boqing Pang(庞博清), Ping Yang(杨平), Bing Xu(许冰)

Chin. Phys. B . 2018, 27(7): 070704. **doi:** 10.1088/1674-1056/27/7/070704

Microwave coherent manipulation of cold atoms in optically induced fictitious magnetic traps on an atom chip

Feng Zhou(周锋), Xiao Li(李潇), Min Ke(柯敏), Jin Wang(王谨), Ming-Sheng Zhan(詹明生)

Chin. Phys. B . 2017, 26(9): 090701. **doi:** 10.1088/1674-1056/26/9/090701

Elastic strain response in the modified phase-field-crystal model

Wenquan Zhou(周文权), Jincheng Wang(王锦程), Zhijun Wang(王志军), Yunhao Huang(黄赟浩), Can Guo(郭灿), Junjie Li(李俊杰), Yaolin Guo(郭耀麟)

Chin. Phys. B . 2017, 26(9): 090702. **doi:** 10.1088/1674-1056/26/9/090702

Raman sideband cooling of rubidium atoms in optical lattice

Chun-Hua Wei(魏春华), Shu-Hua Yan(颜树华)

Chin. Phys. B . 2017, 26(8): 080701. **doi:** 10.1088/1674-1056/26/8/080701

Effect of different bending shapes on thermal properties of flexible light-emitting diode filament*

Liping Wang(王立平)[1], Wenbo Li(李文博)[3], Yichao Xu(徐一超)[1], Bobo Yang(杨波波)[2], Mingming Shi(石明明)[2], Jun Zou (邹军)[2,†], Yang Li(李杨)[1,‡], Xinglu Qian(钱幸璐)[1], Fei Zheng(郑飞)[1], and Lei Yang(杨磊)[3]

[1] *School of Materials Science and Engineering, Shanghai Institute of Technology, Shanghai* 201418, *China*
[2] *School of Science, Shanghai Institute of Technology, Shanghai* 201418, *China*
[3] *Zhejiang Emitting Optoelectronic Technology Co., LTD, Jiaxing* 310000, *China*

(Received 20 June 2018; revised manuscript received 5 September 2018; published online 25 October 2018)

Heat dissipation is an important part of light-emitting diode (LED) filament research and has aroused constant concern. In this paper, we studied the thermal performance of flexible LED filament by numerical simulation and through experiment. The heat dissipation characteristics of spring-like structure flexible LED filament were computed by finite volume method, and it was found that the chip junction temperature was closely related to the pitch and the bending radius. The effect of inclination angle of lighting LED filament was discussed because it is relevant to the spring-like structure flexible LED filament in geometry. The results demonstrated that the temperature of the filament increases as the inclination angle improves.

Keywords: flexible light-emitting diode filament, heat dissipation, numerical simulation, spring-like

PACS: 07.05.Fb, 07.05.TP **DOI:** 10.1088/1674-1056/27/11/110701

1. Introduction

Light-emitting diode (LED) lighting technology has upgraded and improved so quickly that LEDs are now widely used in a wide variety of applications.[1–3] Phosphor-converted light-emitting diodes are the most popular white LED products owing to their high efficiency, low cost, and high reliability.[4–8] In 1997, Nichia made the first commercial white LED all over the world in the manner of light conversion, which was fabricated by coating yellow phosphors on the chip of blue LED. The yellow light emitted by the phosphors was mixed with the blue light from chips into white light.[9] As chip power and luminous efficiency increase every year, LEDs have become a new type of light source. In April 2013, Philips Electronics N.V. announced the release of new products whose luminous efficiency was up to 200 lm/W, which is much higher than the incandescent lamp (100 lm/W) and metal halogen lamp (15 lm/W). Temperature control is one of the most important technologies in modern LEDs.[10–13] It was reported by Arik *et al.*[14,15] that the heat accumulated in chips raised the temperature of PN junction, and this phenomenon led to shorter service life, low color-rendering index, and other issues. Therefore, the heat dissipation problem of LED light sources has become an important factor influencing the LED luminous efficiency and luminous decay.

The packaging methods and materials of LEDs, and the environment that they are used in have a significant influence on the luminous effect. Improving the heat dissipation is a viable approach to enhance the performance of LEDs. There has been a tremendous change in filament technology from tungsten filament to LED filament. During the Guangzhou international lighting exhibition in 2013, only two companies (Shanghai Oppel-LED Co. Ltd and Hangzhou Jingyang Co. Ltd) exhibited LED filament bulbs. In contrast, during the Hong Kong international lighting fair in 2014, there were more than 200 companies exhibiting all kinds of LED filament bulbs. It was reported that more than 600 enterprises produced the LED filaments. The filaments adopted high voltage technology (HVLED) and small current driving technology, which would reduce the heating degree of the light source greatly. Most studies about filament heat dissipation have only focused on the rigid filament, the substrate of which is too hard to bend casually. At the same time, the thermal properties concerning the horizontal placement angle have not been discussed in detail.

Computer numerical simulation technology is an important method for thermal simulation and integrated circuit design.[16] According to Christensen,[17] the heat dissipation performance of LED modules that include a single Lambertian LED and a single chip-on-board (COB) packaged ceramic substrate under different heat dissipation conditions was inves-

*Project supported by the National Natural Science Foundation of China (Grant No. 51302171), Science and Technology Commission of Shanghai Municipality, China (Grant No. 14500503300), Shanghai Municipal Alliance Program, China (Grant No. Lm201547), Shanghai Cooperative Project, China (Grant No. ShanghaiCXY-2013-61), and Jiashan County Technology Program, China (Grant No. 20141316).

†Corresponding author. E-mail: zoujun@sit.edu.cn
‡Corresponding author. E-mail: liyang123@sit.edu.cn

© 2018 Chinese Physical Society and IOP Publishing Ltd

tigated using the finite element method. In this study, a computational model was used to simulate the Philips (E27ES) LED filament bulb. However, most studies on the bulb temperature have only focused on the filling gases and filament substrates, and no single study about the thermal properties on filament shape has been researched.

In this paper, we will analyze the mathematical model of heat conduction and the flexible filament model of convection computer through numerical simulation method, and also the equivalent thermal resistance. The influence of the filament pitch on heat dissipation is also analyzed. At the same time, the temperature of the filament is tested with an infrared temperature measuring instrument, and the result is compared with the numerical simulation.

2. Mathematical modeling

2.1. Experimental setup

The manufacturing process flow of flexible LED filament with a length of 100 mm is shown in Fig. 1. An average of 100 flip-chips was distributed on the copper substrate, the size of which was 200 μm × 510 μm × 250 μm. SY-6021 silicone A (Shenzhen Shenghuayang Electronic Material Co. Ltd), SY-6021 silicone B (Shenzhen Shenghuayang Electronic Material Co. Ltd), $Lu_3Al_5O_{12}$: Ce phosphor (particle size 13 μm, emission band 530 nm, Yinghe in China), (Sr, Ca)$AlSiN_3$: Eu phosphor (emission band 640 nm, Yinghe in China), and (Sr, Ca)$AlSiN_3$: Eu phosphor (emission band 628 nm, Yinghe in China) were used in this study. The insulation was located in the middle of the paste to prevent short circuits of the electrode. When these procedures were finished, a flexible filament could be obtained. In Table 1, the component dimensions of the multiple chip modules and the thermal properties of the encapsulated materials are shown.

Flexible filaments without and with injection currents are shown in Figs. 2(a) and 2(b), respectively. A single chip was extracted to the model according to the symmetry of the package structure, and the temperature field and heat transfer process were calculated when the flexible filament is working. We assume that 80% of the rated power of the filament input is converted into heat energy.[4–7]

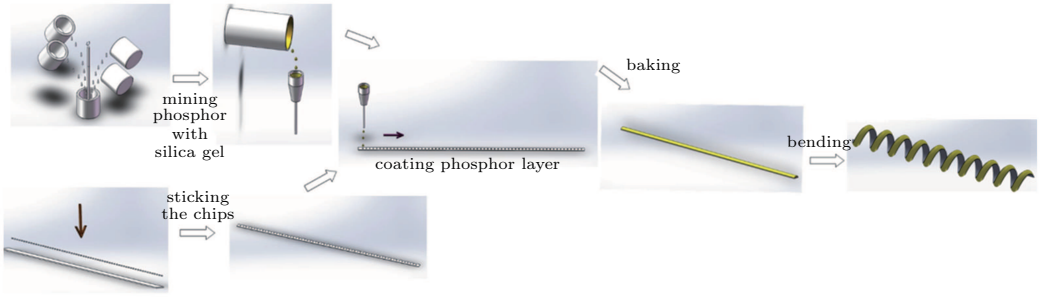


Fig. 1. (color online) Graphic of the process flow of flexible LED filament.

Table 1. Filament module component size and thermal property parameters of packaging materials.

Component	Material	Thermal conductivity/W·m^{-1}·K^{-1}	Size
Chip	sapphire	35	200 μm×510 μm×250 μm
Solder	SnAgCu	58	180 μm×150 μm×200 μm
Phosphor layer	silica glue	0.15	R 2 mm×255 mm
Substrate	Al+Cu+PI	205	255 mm×3 mm×0.15 mm

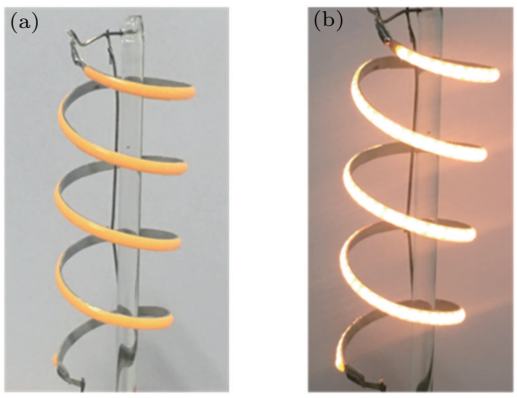


Fig. 2. (color online) Flexible filaments (a) without and (b) with injection currents.

2.2. Geometry

Insulated-metal-substrate (IMS) was used as the power electronic substrate of this LED filament. The flip chips were attached on the substrate through Au–Si eutectic bonding. Finally, the flip chips were attached on the substrate through solder and protected by the phosphor glue. A glass bar was used to support the shape of the flexible filament.

2.3. Model establishment

The following conditions were fulfilled to simplify the calculation process for numerical analysis:

(i) The calculation has a major emphasis on the steady state of thermal system.

(ii) Air density is calculated by the approximate method of Boussinesq.[18]

(iii) Owing to the negligible difference when using temperature-dependent thermal conductivity, the thermal conductivities of all materials are independent of temperature.[19]

(iv) All of the physical properties of air except density are regarded as fixed values.

Conservation of mass, energy, and momentum is the basic equation to solve the energy equation describing the heat and mass transfer of the system. In the calculating model, the mass conservation equation is

$$\frac{\partial(\rho u)}{\partial x}+\frac{\partial(\rho v)}{\partial y}+\frac{\partial(\rho w)}{\partial z}=0, \tag{1}$$

where ρ is the air density, and u, v, and w are the speeds in x, y, and z directions, respectively.

The momentum equation is as follows ($-y$ is the direction of gravity):

$$\begin{aligned} &u\frac{\partial u}{\partial x}+v\frac{\partial u}{\partial y}+w\frac{\partial u}{\partial z}\\ &=-\frac{1}{\rho}\frac{\partial P}{\partial x}+\mu\left(\frac{\partial^2 u}{\partial x^2}+\frac{\partial^2 u}{\partial y^2}+\frac{\partial^2 u}{\partial z^2}\right), \end{aligned} \tag{2}$$

$$\begin{aligned} &u\frac{\partial v}{\partial x}+v\frac{\partial v}{\partial y}+w\frac{\partial v}{\partial z}\\ &=-\frac{1}{\rho}\frac{\partial P}{\partial y}+\mu\left(\frac{\partial^2 v}{\partial x^2}+\frac{\partial^2 v}{\partial y^2}+\frac{\partial^2 v}{\partial z^2}\right)-g\left[1-\beta\left(T-T_0\right)\right], \end{aligned} \tag{3}$$

$$\begin{aligned} &u\frac{\partial w}{\partial x}+v\frac{\partial w}{\partial y}+w\frac{\partial w}{\partial z}\\ &=-\frac{1}{\rho}\frac{\partial P}{\partial z}+\mu\left(\frac{\partial^2 w}{\partial x^2}+\frac{\partial^2 w}{\partial y^2}+\frac{\partial^2 w}{\partial z^2}\right), \end{aligned} \tag{4}$$

where P is the pressure of gas, μ is the viscosity of air, g is the acceleration of free fall, and β is the air expansion coefficient. The energy conservation equation is

$$u\frac{\partial T}{\partial x}+v\frac{\partial T}{\partial y}+w\frac{\partial T}{\partial z}=\frac{1}{\rho}\frac{k}{c_{\mathrm{p}}}\left(\frac{\partial^2 T}{\partial x^2}+\frac{\partial^2 T}{\partial y^2}+\frac{\partial^2 T}{\partial z^2}\right), \tag{5}$$

where k is the thermal conductivity, c_{p} is the specific heat at constant pressure.

The air density is calculated by the approximate method of Boussinesq

$$\rho-\rho_0=-\rho_0\beta(T-T_0), \tag{6}$$

where ρ_0 is the air density at room temperature.

Heat can be delivered by convection, radiation, and thermal conduction. Heat is delivered by thermal conduction mainly in solid state. In the interfacial region, heat is delivered in the way of convection. In fluids, both thermal conduction and convection exist at the same time. Radiation could be emitted from solid surface to the colder outside by means of electromagnetic wave. The packaging model and boundary conditions are shown in Fig. 3. The other faces are open boundaries for environmental temperature and environmental pressure. The junction temperature of chips is taken as the monitoring point. The other coefficients of heat transfer could be calculated under the coupling condition between solid and fluid. Assuming that T_{a} is the environmental temperature at 25 °C, τ is the direction of heat transfer, then the Fourier's law is

$$Q=-kA\frac{\partial T}{\partial \tau}, \tag{7}$$

where k is the thermal conductivity, and A is the surface area of the filament.

Convection exists in the region between filament model and air. Newton cooling formula is

$$Q=hA(T-T_{\mathrm{a}}), \tag{8}$$

where h is the convection heat transfer coefficient.

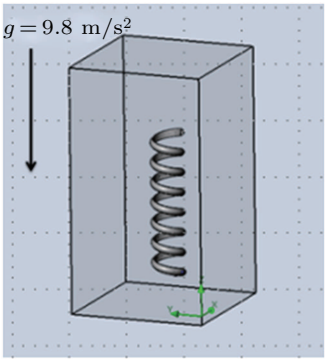


Fig. 3. (color online) Flexible filament module and boundary conditions.

2.4. Numerical procedure and validation

Figure 4 shows the numerical model of solder, single chip, substrate, and phosphor layer of the package module. These models are designed in real size. The temperature field and heat transfer process at working state are calculated.

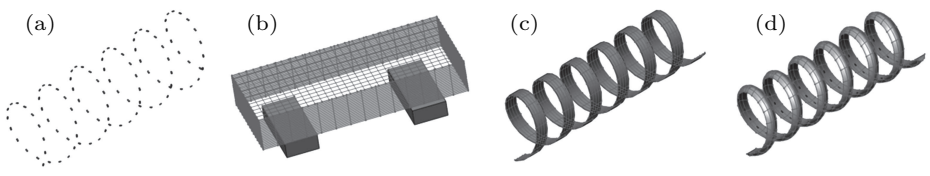


Fig. 4. (a) Solder, (b) chip, (c) substrate, and (d) phosphor layer.

2.5. Mesh and boundary conditions

As shown in Fig. 4, there are four sub-domains included in the computational domain; i.e., chips, aluminum substrate (Al substrate), phosphor layer (glue), and also gas outside the filament. The outside cuboid enveloping the filament is included to simulate the heat change between the filament and the ambient. Heat conduction, natural convection, and radiation heat transfer are involved in the problem. Standard heat conduction equation is used for heat transfer in solid domains such as chips, substrate, and glue. Navier–Stokes equations with buoyancy force term are used for natural convection outside the filament. Figures 5(a) and 5(b) show the multi-block unstructured meshes which are generated by FLOEFD 15.0 in all domains. Chips are distributed on the filament substrate evenly. Figure 5(c) shows the physical model of the computational domain clearly according to the side view.

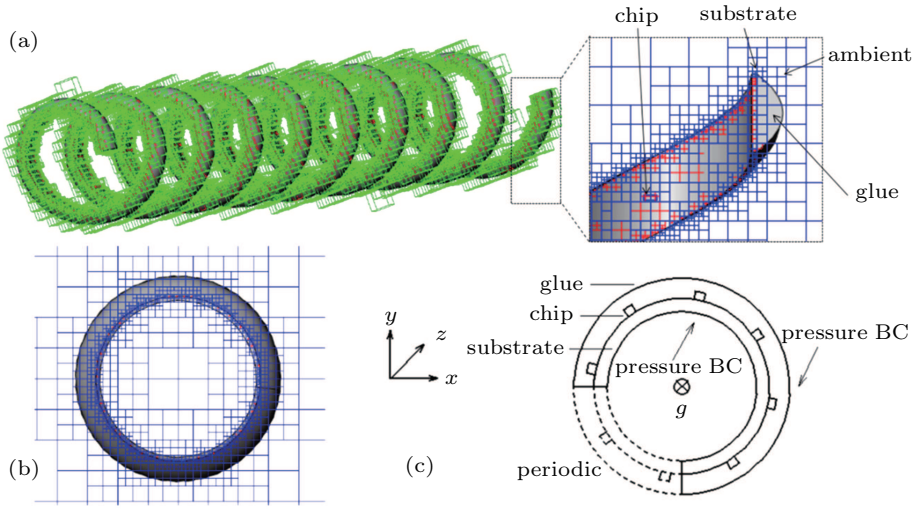


Fig. 5. (color online) Numerical simulation model: (a) mesh, (b) side view, and (c) the physical model of the computational domain.

3. Results and discussion

3.1. The effect of a spring-like filament pitch

Figure 6 shows the thermal distribution of the spring-like LED filaments at different pitches. In Fig. 6, we have demonstrated that the highest filament temperature decreases widely by increasing the stretching pitch while the lowest temperature is almost constant. Compared with straight filament, the heat generated by the multi-chips of cylinder screw distribution is more severe owing to the closer distribution, which prevents heat from spreading outward.

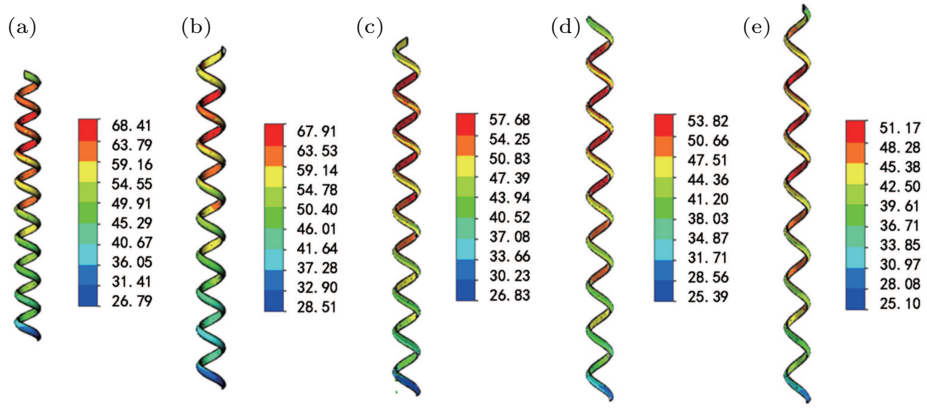


Fig. 6. (color online) Thermal distribution of filaments at different stretching pitches by simulation.

3.2. The effect of a spring-like filament bending radius

The result of the thermal distribution of the filament at different stretching pitches by infrared test is shown in Fig. 7. It can be seen that the highest filament temperature decreases widely by increasing the stretching pitch while the lowest temperature is almost constant, which agrees with the simulation result as shown in Fig. 6. The thermal conductivity of the substrate is higher than that of the silica. Thus, it is expected that this will result in the higher temperature of substrate than that of phosphor silica.

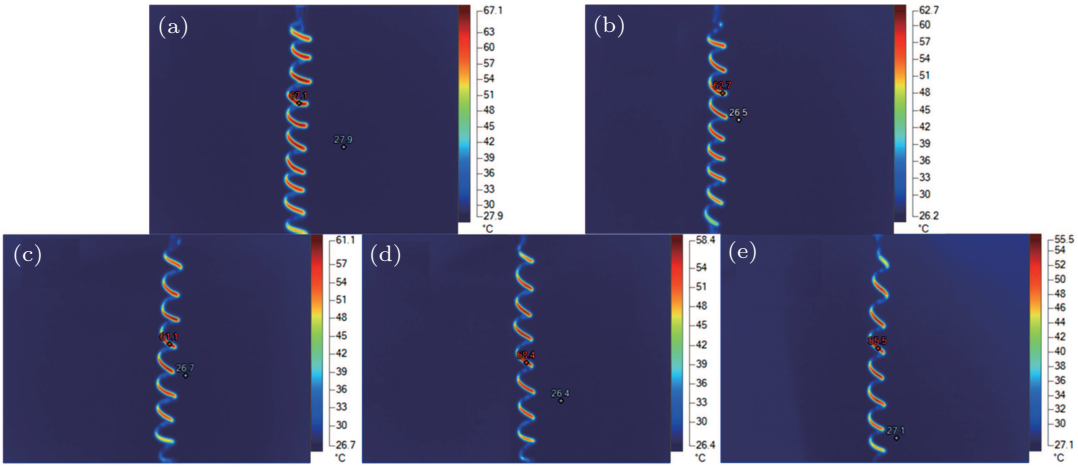


Fig. 7. (color online) Thermal distribution of filaments at different stretching pitches by infrared test.

By combining Figs. 6 and 7, we can draw the conclusion that the highest temperature point is the upper part on the filament, but not the top. The larger the pitch, the longer the high temperature part, and the lower the air heat density. This indicates that a larger pitch results in a lower filament temperature.

Figure 8 further illustrates the highest temperature and lowest temperature of the filament by simulation and infrared test under different pitches (measured at a typical injected power of 3.5 W) from 11 mm to 19 mm. It is evident that the highest temperature of both simulation and infrared test decreases with the increase of the filament pitch, while it is opposite for the lowest temperature. This indicates that a larger pitch benefits the heat dissipation, whereas it simultaneously increases the heat exchange area surface between air and filament. Furthermore, the ambient temperature is responsible for the lowest temperature of filament. Some reasonable reasons behind these results are provided.

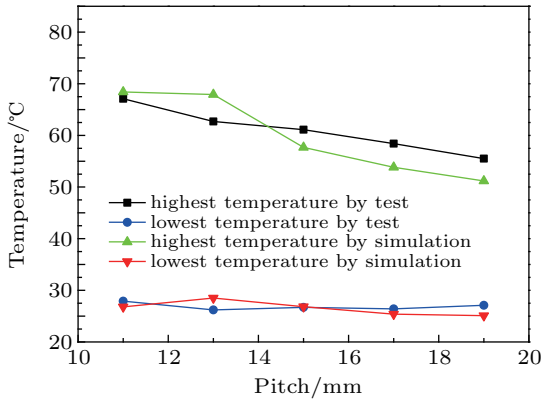


Fig. 8. (color online) Highest temperature and lowest temperature of filament by simulation and infrared test under different pitches.

3.3. The effect of the filament inclination angle

The spiral line can be understood as a complex movement of the particle, together with circular motion and straight motion, as shown in Fig. 9. The ratio of pitch to radius eventually affects the helix angle. The temperature distribution of simulated straight filaments at different inclination angles is depicted in Fig. 10. It can be seen that the highest filament temperature increases widely by increasing the inclination angle, while the lowest temperature is almost constant.

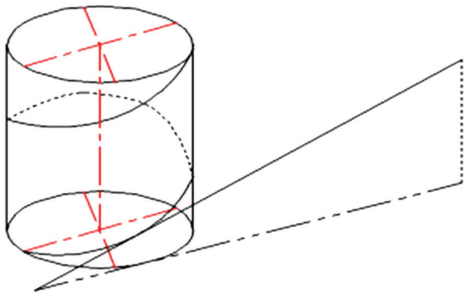


Fig. 9. (color online) Sketch of spiral filament expansion.

Figure 11 shows the corresponding relation of the highest temperature under different inclination angles, in which the black squares correspond to the maximum temperatures in Figs. 10(b)–10(f).

3.4. The thermal resistance of the LED filament model

Thermal resistance is an important parameter to measure the performance of heat dissipation. The model can be calculated under the total power of 3.5 W through Eq. (9). The thermal resistance of the filament is the thermal resistance of multi-chips ranging in parallel. The total thermal resistance is reduced with the increase of the number of chips. Multi-chips in parallel increase the contact area, resulting in the reduction of the thermal resistance. It means that at a constant input power, the more chips, the better the heat dissipation, which can be calculated through Eq. (10).

There are 4 basic steps of the heat transfer: (I) from chips to glue; (II) from chips to substrate; (III) from glue to ambient; (IV) from substrate to ambient. Each step is closely related to one or more thermal resistance models.

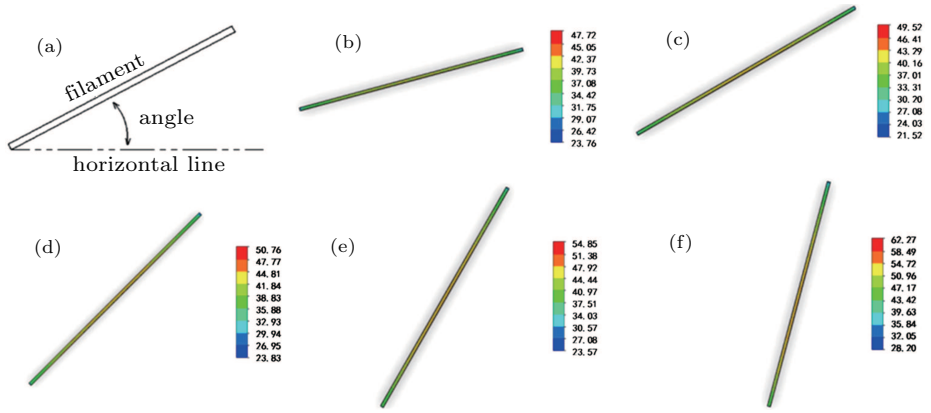


Fig. 10. (color online) (a) Schematic diagram of the inclination angle. (b)–(f) Thermal distribution of filaments at different inclination angles by simulation.

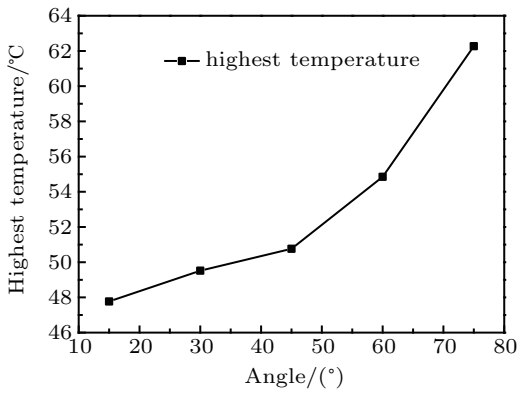


Fig. 11. Corresponding relation of the highest temperature under different inclination angles.

There may be thermal contact resistance at the interface between chips and glue, chips and substrate in step (I), and also a spreading thermal resistance when heat is transferred from chips to glue or from chips to substrate. It is difficult to accurately analyze the spreading thermal resistance owing to the complex structure of the filament. The thermal resistances concerning step (I) are not covered in the discussed thermal resistance network and, therefore, the suggested model is only capable of predicting the average filament temperature.

When heat is transferred from the glue or substrate to the ambient in step (II), it is partly transferred by natural convection and partly through radiation, associated with the convective resistance and radiative resistance, respectively. There is only conduction in the heat transfer process of glue and substrate, corresponding to the conductive resistance.

The thermal resistant network, beginning from the junction temperature and ending at the ambient temperature, is shown in Fig. 12, where T_a is the ambient temperature, R_{NC} is the convective resistance, R_{rad} is the radiative resistance, $R_{glue,cond}$ is the conductive resistance of glue, T_j is the temperature of PN junction, $R_{Al,cond}$ is the conductive resistance of substrate, and R_{c-p} is the thermal resistance of chip.

The total thermal resistance R is

$$R = \frac{T_j - T_a}{P}, \tag{9}$$

$$R = \frac{\delta}{A\lambda}, \tag{10}$$

where δ is the average thickness of substrate and glue.

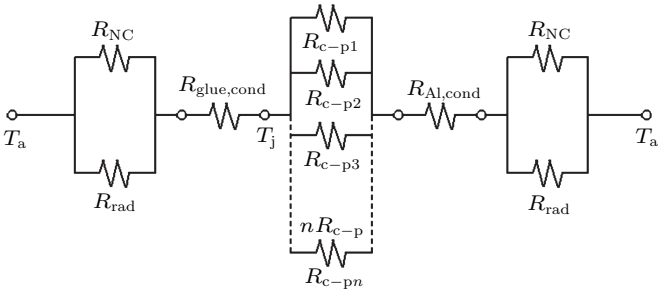


Fig. 12. Schematic diagram of thermal resistance model for LED filament.

4. Conclusion

In summary, the shape of flexible LED filament has a significant influence on the heat dissipation of spring-like structure flexible LED filament. The junction temperature of the chip is closely related to the pitch and the bending radius. The results demonstrate that the temperature of the filament increases as the inclination angle improves. It can also be calculated that if more chips are distributed at a constant input power, then the heat dissipation will be better.

Appendix A: Governing equations

The following assumptions are made to simplify the calculations:

(A) One-dimensional heat conduction based on Fourier's law;

(B) The temperature outside the filament is the same as the ambient temperature;

(C) The heat generated in the LED chips is symmetric and uniform;

(D) Gravity has no effect on the heat transfer.

The governing equations are as follows:

Continuity equation

$$\frac{\partial \rho}{\partial t}+\frac{\partial(\rho u)}{\partial x}+\frac{\partial(\rho v)}{\partial y}=0,$$

where ρ is the air density, and u and v are the velocities in the x and y directions.

Momentum equations

$$P\left(\frac{\partial u}{\partial t}+u\frac{\partial u}{\partial x}+v\frac{\partial u}{\partial y}\right)=u\left(\frac{\partial^2 u}{\partial x^2}+\frac{\partial^2 u}{\partial y^2}\right)-\frac{\partial P}{\partial x}+S_u,$$

$$P\left(\frac{\partial v}{\partial t}+u\frac{\partial v}{\partial x}+v\frac{\partial v}{\partial y}\right)=v\left(\frac{\partial^2 v}{\partial x^2}+\frac{\partial^2 v}{\partial y^2}\right)-\frac{\partial P}{\partial y}+S_v,$$

where S_u and S_v represent the appropriate sink terms which account for the pressure drop caused by the solid material.

Energy equation

$$P\left[\frac{\partial H}{\partial t}+u\frac{\partial H}{\partial x}+v\frac{\partial H}{\partial y}\right]=\frac{k}{c_{\mathrm{P}}}\left[\frac{\partial^2 H}{\partial x^2}+\frac{\partial^2 H}{\partial y^2}\right]+S_n,$$

where H represents the specific enthalpy and S_n is the heat generation rate

$$S_n=\frac{\rho}{c_{\mathrm{p}}}\frac{\partial(\Delta H)}{\partial t}.$$

References

[1] Liu S and Luo X B 2011 *LED Packaging for Lighting Applications: Design, Manufacturing and Testing* (Singapore: Wiley)

[2] Krames M R, Shchekin O B, Mueller-Mach R, Mueller G O, Zhou L, Harbers G and Craford M G 2007 *J. Disp. Technol.* **3** 160

[3] Schubert E F and Kim J K 2005 *Science* **308** 1274

[4] Ma Y, Hu R, Yu X, Shu W and Luo X 2017 *Int. J. Heat Mass Transfer* **106** 1

[5] Abdelmlek K B, Araoud Z, Ghnay R, Abderrazak K, Charrada K and Zissis G 2016 *Appl. Therm. Eng.* **102** 251

[6] Chhajed S, Xi Y, Li Y L, Gessmann T and Schubert E F 2005 *J. Appl. Phys.* **97** 054506

[7] Ye H, Mihailovic M, Wong C K Y, van Zeijla H W, Gielen A W J, Zhang G Q and Sarroa P M 2013 *Appl. Therm. Eng.* **52** 353

[8] Xie B, Hu R and Luo X 2016 *J. Electron. Packag.* **138** 020803

[9] Nakamura S and Fasol G 1997 *Blue Laser Diode: GaN Based Light Emitters Lasers* (Berlin: Springer-Verlag) pp. 16–20

[10] Xu H Y, Chen X F, Peng Y, Xu M S, Shen Y, Hu X B and Xu X G 2015 *Chin. Phys. B* **24** 067305

[11] Qi W J, Zhang M, Pan S, Wang X L, Zhang J L and Jiang F Y 2016 *Acta Phys. Sin.* 65 077801 (in Chinese)

[12] Norazlina M S, Dheepan Chakravarthii M K, Shanmugan S, Mutharasu D and Shahrom M 2017 *Chin. Phys. B* **26** 098901

[13] Chen H T, Lü Y J, Gao Y L, Chen Z, Zhuang R R, Zhou X F and Zhou H 2012 *Acta Phys. Sin.* **61** 167104 (in Chinese)

[14] Arik M, Becker C, Weaver S and Petroski J 2004 *Proc. SPIE* **5187** 64

[15] Ma L, Yang Y and Liu J 2013 *Heat Mass Transfer* **49** 85

[16] Tian L X, Wen S S, Yao R H, Chen Y C and Xie J N 2014 *Acta Opt. Sin.* **34** 1123002 (in Chinese)

[17] Christensen A and Graham S 2009 *Appl. Therm. Eng.* **29** 364

[18] Joo Y H and Kim S J 2015 *Int. J. Heat Mass Transfer* **83** 345

[19] Ha M S 2009 *Thermal Analysis of High Power LED Arrays* (MS Thesis) (Atlanta: Georgia Institute of Technology)